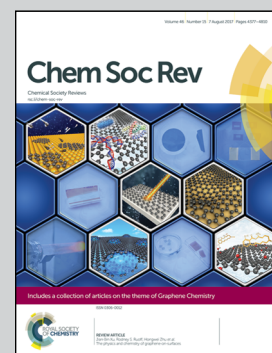


Featuring work from the research groups of Professor Martin Pumera, Nanyang Technological University, Singapore and Professor Zdeněk Sofer, University of Chemistry and Technology, Czech Republic. This research is supported by the National Research Foundation, Prime Minister's Office, Singapore under its CREATE programme, by the Neuron Foundation for science support and by Czech Science Foundation (GACR No. 15-09001S and 16-05167S).

Towards stoichiometric analogues of graphene: graphane, fluorographene, graphol, graphene acid and others

Hydrogenated graphene (graphene), fluorographene, hydroxygraphene (graphol), thiographene, cyanographene, aminographene, graphene acid pose unique and well defined chemical and physical properties, allowing their further transformation and application in the devices.

### As featured in:



See Martin Pumera and Zdeněk Sofer,  
*Chem. Soc. Rev.*, 2017, **46**, 4450.



Cite this: *Chem. Soc. Rev.*, 2017, **46**, 4450

Received 24th March 2017

DOI: 10.1039/c7cs00215g

[rsc.li/chem-soc-rev](http://rsc.li/chem-soc-rev)

## Towards stoichiometric analogues of graphene: graphane, fluorographene, graphol, graphene acid and others

Martin Pumera \*<sup>a</sup> and Zdeněk Sofer \*<sup>b</sup>

Stoichiometric derivatives of graphene, having well-defined chemical structure and well-defined chemical bonds, are of a great interest to the 2D materials research. Hydrogenated graphene (graphene), fluorographene, hydroxygraphene (graphol), thiographene, cyanographene, aminographene, graphene acid pose unique and well defined chemical and physical properties, allowing their further transformation and application in the devices. Here we overview various methods of their synthesis and discuss their chemistry and properties. It is expected that the family of stoichiometric derivatives of graphene will grow beyond listed examples in the near future.

### 1. Introduction

According to the IUPAC definition, graphene is, at least in its idealized form, “a single carbon layer of the graphite structure, describing its nature by analogy to a polycyclic aromatic hydrocarbon of quasi-infinite size”.<sup>1</sup> In the last decade, graphene has become a highly popular 2-dimensional material.<sup>2–6</sup> It has an

<sup>a</sup> Division of Chemistry & Biological Chemistry, School of Physical and Mathematical Sciences, Nanyang Technological University, Singapore 637371, Singapore. E-mail: pumera.research@gmail.com; Fax: (+65) 6791-1961

<sup>b</sup> Department of Inorganic Chemistry, University of Chemistry and Technology Prague, Technická 5, 166 28 Prague 6, Czech Republic. E-mail: zdenek.sofe@vscht.cz



**Martin Pumera**

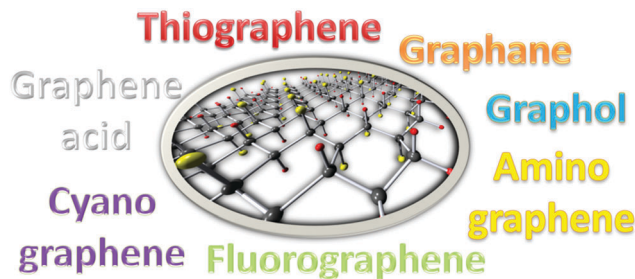
Prof. Martin Pumera is a tenured faculty member at Nanyang Technological University, Singapore since 2010. He received his PhD at Charles University, Czech Republic, in 2001. After two postdoctoral stays (in the USA, Spain), he joined the National Institute for Materials Science, Japan, in 2006 for a tenure-track arrangement and stayed there until Spring 2008 when he accepted a tenured position at NIMS. In 2009, Prof. Pumera received a ERC-StG award. Prof. Pumera has broad interests in nanomaterials and microsystems, in the specific areas of electrochemistry and synthetic chemistry of 2D materials and micro and nanomachines. He is Editor-in-Chief of *Applied Materials Today* (Elsevier; CiteScore 5.71), member of Editorial board of *Chem. Eur. J.*, *Electrochem. Commun.*, *Electrophoresis*, *Electroanalysis*, *The Chemical Records*, *ChemElectroChem* and eight other journals. He has published over 470 articles, which received over 18 000 citations (h-index of 68).



**Zdeněk Sofer**

Prof. Zdeněk Sofer is an Associated Professor at the University of Chemistry and Technology Prague since 2013. He received his PhD also at University of Chemistry and Technology Prague, Czech Republic, in 2008. During his PhD he spent one year in Forschungszentrum Jülich (Peter Grünberg Institute, Germany) and also one postdoctoral stay at University Duisburg-Essen, Germany. Research interests of Prof. Sofer concerning on nanomaterials graphene based materials and other 2D materials, its chemical modifications and electrochemistry. He is member of Editorial board of *FlameChem*. He has published over 240 articles, which received over 3500 citations (h-index of 31).





Scheme 1 Well defined stoichiometric derivatives of graphene are on the frontiers of graphene research.

very simple structure (it is a large polycyclic aromatic carbon molecule) of atomic thickness. Many materials scientists, physicists, and chemists are exploring its structure. There is a large number of chemical derivatives of graphene. Most commonly known is graphene oxide. While the name suggests that there will be a well-defined bonding arrangement in the structure with well-defined stoichiometry, as most inorganic oxides have, the opposite is true. The structure of graphene oxide has not been known in detail until now and several structural models exist.<sup>136</sup> Graphene oxide consists of a wide variety of carbon–oxygen bond arrangements, such as alcohol, carbonyl, carboxyl, ether, and ester. Their abundance depends on the preparation route.<sup>137</sup> Therefore, it should not be surprising that the original articles on graphite oxide (stacked graphene oxide) referred to this material as graphite oxide/hydroxide or graphite acid (to reflect its acidic character). Other chemical derivatives of graphene are, for example, doped graphenes (most commonly N-doped graphenes) where again, a variety of carbon–nitrogen bonds exist and the amount of nitrogen is usually very low and non-stoichiometric.

In this article, we wish to review different derivatives of graphene. We wish to focus on derivatives with well-defined stoichiometry and structure. These include graphane, fluorographene, and others with a general formula of  $C_1X_{1-\delta}$ , where X is a heteroatom or functional group such as H, halogen, -OH, -SH, -COOH, or combinations of previous groups ( $C_1X_aY_{1-a}$ ) (see Scheme 1). The attempts of creating well defined derivatives of graphene with nitrogen will be reviewed as well.

## 2. Monoatomic derivatives (C–X): graphane and halogen graphenes

The addition of hydrogen or halogen atoms onto the graphene skeleton leads to monoatomic derivatives of graphene with a simple structure consisting of single-bonded heteroatoms (for the purpose of this review, any atom other than carbon is considered a heteroatom) to carbon. It should be noted that the chemical properties of hydrogen are much closer to those of the halogen group than to those of group IA (alkaline metals), which is documented by the fact that hydrogen is among the group VIIA elements in many older periodical table systems. Addition of a monovalent atom leads to a non-ambiguous structure (as when N, B, S, or O are added to a graphene

backbone as several types of arrangements can exist with these multivalent atoms).

Addition of monovalent heteroatoms to aromatic carbon rings in graphene leads to a disturbance of aromaticity; the thickness of the material is no longer monoatomic as additional atomic layers are added by the heteroatom. In addition, the basic  $C_6$  skeleton is not planar as in graphene but buckled. One can demonstrate this in the case of planar benzene and buckled cyclohexane or hexachlorocyclohexane. This leads into band gap opening, charge separation, and possible ferromagnetic ordering, different interlayer forces, catalytic effects, and so on. First, we shall discuss hydrogenated graphene and later on we will move to the area of halogenated graphenes.

### 2.1. Graphane

Fully hydrogenated graphene is a wide band gap semiconductor with a predicted value of 3.5 eV for the chair conformation and 3.7 eV for the boat conformation.<sup>7,8</sup> Band gap is strongly dependent on hydrogen content, which can be used for its tuning. The electronic structure can be further controlled by geometry, such as the formation of nanoribbons.<sup>9</sup> These interesting properties open a huge potential of this material in current micro- and optoelectronics. The properties of graphane can also be controlled by its interaction with various metallic ions. Several theoretical studies were performed for such systems.<sup>10</sup> The presence of ferromagnetic ordering was also experimentally observed within highly hydrogenated graphene.<sup>11</sup> Graphane also has several other possible applications including hydrogen storage, electrochemical storage, and conversion devices as well as sensing applications.

There are several methods of preparing graphane (summary formula  $C_1H_1$ ) or highly hydrogenated graphene ( $C_1H_{1-\delta}$ ). In principle, there are three basic conceptual methods. Hydrogenation can be accomplished (a) *via* low-pressure  $H_2$  plasma, (b) high-pressure  $H_2$  atmosphere, or (c) *via* wet chemistry (solution) based approaches. Hydrogenation of graphene to graphane in low-pressure plasma was first introduced in 2009.<sup>138</sup> Because of the low sample amount in this original work, the exact level of hydrogenation was not determined. This first work was followed by several variations, *i.e.*, hydrogenation of CVD graphene with hydrogen content under 10%.<sup>139</sup> While it was assumed that hydrogenation occurs on only one side of CVD graphene when attached to a substrate, hydrogenation of epitaxial graphene with  $H_2$  and  $D_2$  led to hydrogenation from both sides of a graphene sheet.<sup>140</sup> Hydrogen plasma was also applied for the bulk synthesis of hydrogenated graphene, but the degree of hydrogenation was also relatively low. For example, hydrogenation of graphene oxide in microwave plasma led to hydrogenation efficiencies of 10–12%.<sup>141</sup>

In industry, aromatic hydrocarbon hydrogenation occurs under high pressure and elevated temperature to drive the reaction of alkene  $H_2C=CH_2 + H_2 \rightarrow H_3C-CH_3$  in the presence of a Ni, Pd, or Pt catalyst. However, when performed on graphene oxide with pressures of up to 150 bar and temperatures of up to 500 °C, the hydrogenation efficiency scarcely reached 3.7%.<sup>142</sup> Another high-pressure method was devised by the hydrogenation



of graphene on Cu foil in an Anvil (diamond) cell under pressure of 2.6–5 GPa in the presence of molecular hydrogen.<sup>12</sup> High-pressure hydrogenation was also applied to CVD-grown graphene. However, the exact degree of hydrogenation was not reported. Hydrogenated graphene was also further derivatized because of its extended reactivity in comparison with unmodified graphene.<sup>13</sup>

Wet chemistry hydrogenation can be carried out in either aqueous or non-aqueous media. In the first category, the hydrogenation of graphene oxide with nascent hydrogen ( $H^\bullet$ ) generated from a reaction of HCl with metal leads to 10% hydrogenation.<sup>14</sup> Typically, the wet chemical methods are based on the reduction of oxygen functionalities present on the graphene oxide surface. Typically, ketone and carboxylic acids can be reduced to hydroxyls together with carbon atom hydrogenation. Several reducing reagents like complex hydrides can be used for such hydrogenation. The hydrogenation was proofed by deuterium labeling.<sup>15</sup> In general, many types of chemical reductions of graphene oxide can lead to partial hydrogenation.

Non-aqueous methods include the so called Birch hydrogenation reaction, a method that can be employed to hydrogenate graphene (Fig. 1)<sup>16,17</sup> and graphene oxide,<sup>11</sup> with efficiency ranging from 70% to 114% (meaning that hydrogenated graphene (graphane) had a summary formula of  $C_1H_{1.14}$ ). This is due to the small size of the graphene sheets and the presence of defects, which can contain  $-CH_2$  and  $-CH_3$  groups (similarly to fluorographene, see below).<sup>18</sup> Hydrogenation of carbon nanotubes *via* the Birch method, which leads to graphane nanostripes with enhanced magnetic properties, was also highly effective.<sup>19</sup> The Birch reaction is carried out in liquid ammonia, in which alkali metal such as Li, Na, K, or Cs is dissolved and which acts as a source of solvated electrons, which are transferred to the graphene. Such graphene subsequently reacts with a proton source, which can be alcohol (methanol, ethanol, or propanol) or water.<sup>20</sup> For single-layer graphene, it has been shown that hydrogenation takes place uniformly across the sheet while for few-layer graphene (FLG) hydrogenation was not observed on

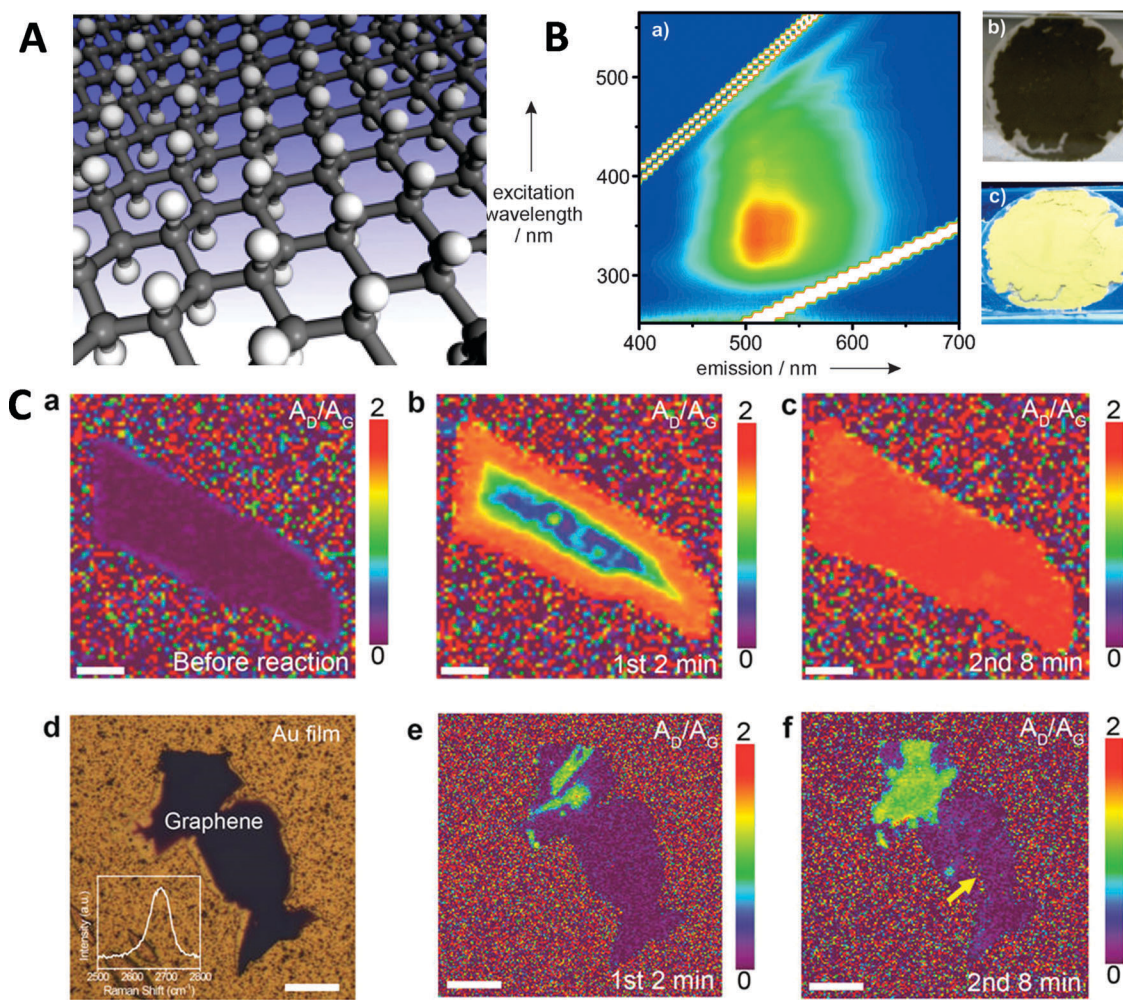


**Fig. 1** Graphane. (A) Structure of fully hydrogenated graphene (graphane). Reproduced from ref. 7 with permission from American Physical Society, copyright 2007. (B) Fluorescence of hydrogenated graphene. Reproduced from ref. 17 with permission from Wiley-VCH, copyright 2013. (C) Mechanism of the Birch hydrogenation elucidated. Time evolution of Raman  $A_D/A_G$  (defects/graphitic carbon) upon exposure to Li in liquid  $NH_3$  for bilayer graphene (a–c) and few layer graphene with closed edges (d–f) shows that hydrogenation of bilayer structure starts at the edges. Reproduced from ref. 21 with permission from American Chemical Society, copyright 2017.



materials with sealed edges. This suggests that hydrogenation takes place from the defect/edge points of FLG, possibly *via* alkali metal intercalation (Fig. 1).<sup>21</sup> Highly hydrogenated graphene is reactive and it is possible to further functionalize it *via* a standard chemical reaction on remaining allyl bonds.<sup>22</sup> The Birch method can be utilized on halogenated graphenes, which leads to high levels of hydrogenation—up to 7.5 wt% of hydrogen.<sup>23</sup> This exceeds the DOE limits for hydrogen storage materials for automotive applications (5.5 wt%) and such materials, coupled with an appropriate recycling system, can be utilized as safe (compared to Mg or Li hydrides) hydrogen storage material. Another non-aqueous method utilizes graphite intercalation compounds with K (prepared in THF) with subsequent protonation with alcohols or water. This leads into tunable hydrogenation with a hydrogen content up to 66%.<sup>24</sup>

The material properties of graphane and highly hydrogenated graphene are much different from those of graphene. Hydrogenation opens a band gap of up to 3.7 eV,<sup>8</sup> depending on the hydrogenation level and conformation. This leads to the fluorescence of highly hydrogenated graphene (Fig. 1).<sup>17</sup> Partial hydrogenation leads to localized and unpaired electrons of non-hydrogenated carbon atoms which, in turn, leads to  $sp^3$  carbon-induced ferromagnetism.<sup>11,25</sup> These properties are also

seen in other monovalent atom/group functionalized graphenes, as described below. Graphane was not found to have special electrocatalytic properties,<sup>26</sup> unless paired with metal nanoparticles.<sup>12</sup>

## 2.2. Halogen graphenes

Compared to other graphene derivatives, halogenated and especially fluorinated graphene exhibits several different properties. These differences originate from the high differences in the electronegativity of individual heteroatoms. In comparison with hydrogenated graphene, its fluorinated counterpart is more broadly available since it can be prepared by “bottom-up” as well as “top-down” methods. High electronegativity leads to the band-gap opening and fluorographene can act as an insulator in layered material heterostructures. Fluorographene is also well known for its several outstanding properties such as large negative magnetoresistance, high optical transparency and electrical band gap exceeding values reported to be about 3.8 eV (Fig. 2).<sup>27–33,41,42</sup> Fluorographene also has good thermal stability. Theoretical calculations show the strong influence of fluorographene conformation on band gap structure and energy. Theoretical calculations of fluorinated graphene with low fluorine concentrations (below  $CF_{0.125}$ ) show the polar character of the C-F bond and lead to the metallic conductivity of such material.<sup>33</sup>

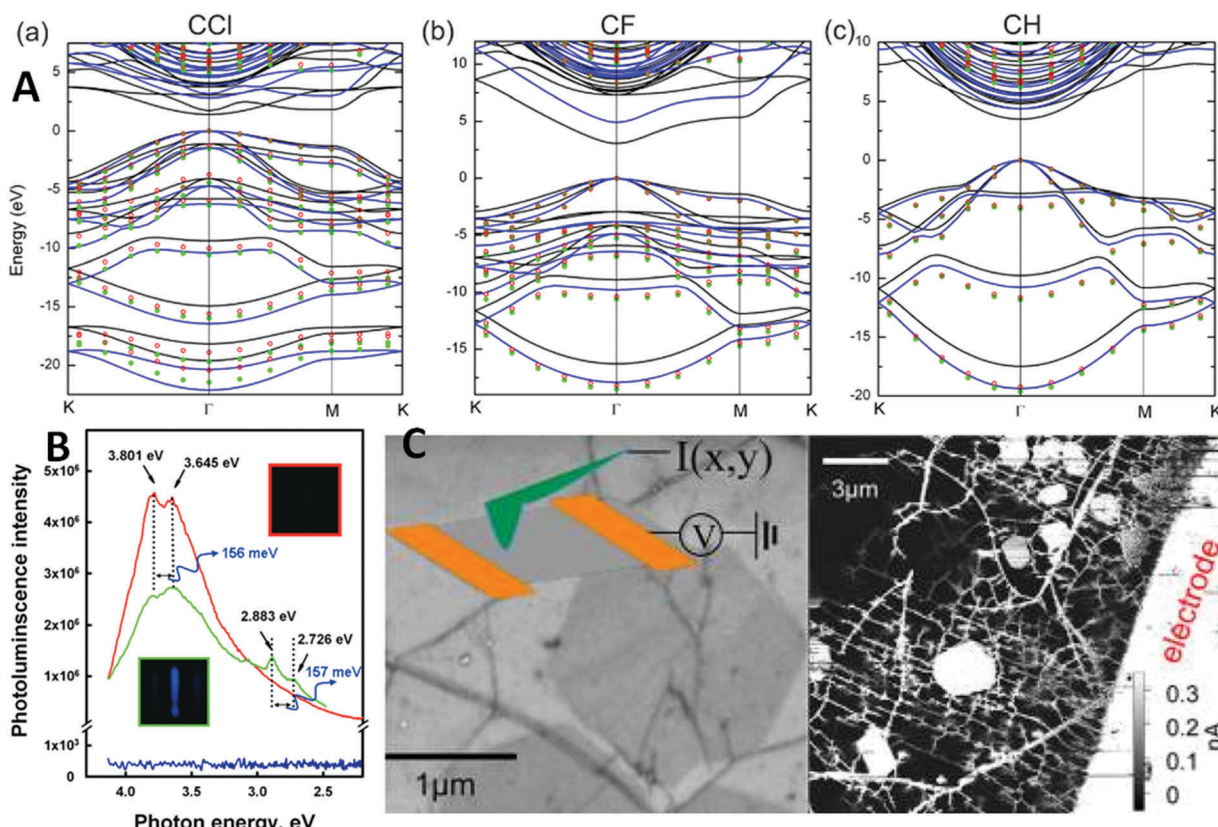


Fig. 2 (A) The electronic band structure in the vicinity of the band gap for fluorographene as well as its counterparts (chlorographene and graphane). Reprinted from ref. 41 with permission from American Chemical Society, copyright 2013; (B) room temperature photoluminescence emission of the pristine graphene and fluorographene dispersed in acetone using 290 nm (4.275 eV) excitation shows luminescence maxima at about 3.8 eV. Reproduced from ref. 42 with permission from American Chemical Society, copyright 2011. (C) Fluorographene was deemed to be insulator; however, it has been shown that it is conducting material due to the conducting islands. Reproduced from ref. 43 with permission from American Chemical Society, copyright 2014.



A higher degree of fluorination leads to large changes in electron density and band gap opening. With a composition of  $\text{CF}_{0.25}$ , graphene shows a wide band gap with energy of 2.92 eV based on GGA calculations.<sup>33</sup> Band gap can also be controlled by various conformations of stoichiometric fluorographene: twist-boat, boat, and stirrup conformations show band gaps of 3.05 eV, 3.28 eV, and 3.58 eV, respectively.<sup>29</sup> The band gap value is strongly dependent on composition and its value can be tuned by the degree of fluorination. Fluorographene is well known for its extremely hydrophobic behavior. Therefore, self-cleaning surfaces, hydrophobic coatings as well as self-lubricating surfaces all fall within its potential applications. Fluorographene has excellent potential for application in primary batteries paired with lithium. Fluorographene acts as a cathode material with excellent long-term stability and a theoretical energy density of 2162 W h kg<sup>-1</sup> with a theoretical electromotive force of 4.57 V.<sup>34,35</sup> Other applications including the use of magnetic resonance imaging were reported.<sup>36</sup> Unlike diamagnetic graphene, its fully fluorinated counterparts exhibit paramagnetism.<sup>37</sup> The ferromagnetism reported for partially fluorinated graphene is usually related to the magnetism of fluorine atoms on defects and edge sites.<sup>38</sup> Tang reported the relationship of magnetic behavior to fluorographene conformation structure as well as tensile strain.<sup>39</sup> While fluorinated graphene was deemed to be insulator at first,<sup>27</sup> it was shown that it is actually conducting material (Fig. 2C) due to conducting paths in its crystal,<sup>43</sup> excellent for electrode fabrication.<sup>40</sup>

Compared to fluorographene, all its other halogenated counterparts are unstable and their overall stoichiometric composition was never reported.<sup>31,32,44-46</sup> Fluorinated graphene decomposes at temperatures around 400 °C and is accompanied by partial restoration of graphene structure.<sup>27,28,47</sup> Graphene etching was also observed at higher temperatures.<sup>27,48</sup> These processes were studied by Raman spectroscopy as well as through high-temperature electrical conductivity measurements and analysis of formed gaseous products by GC-MS. Detailed high-temperature measurements of electrical conductivity show excellent insulating properties up to 350 °C.<sup>27,49</sup> Chemical methods such as reaction with potassium iodide or hydrazine can also be used for removing fluorine from fluorographene.<sup>28,30</sup> Light-induced removal of fluorine from fluorographene was also reported in the literature.

Both general synthetic strategies based on “bottom-up” and “top-down” synthesis can be applied for the bulk synthesis of fluorographene. This is due to the commercial availability of fluorinated graphite (fluorographite) bulk with a controlled amount of fluorine. Fluorographite was commercially available from the middle of the 20th century and the concentration of fluorine can be controlled by experimental conditions (temperature and partial pressure of fluorine) during the reaction. Since the methods of mechanical “top-down” synthesis are well known for graphene synthesis, it can also be simply transferred for fluorographene. This method offers a simple and scalable procedure for fluorographene synthesis (Fig. 3A). Also, the mechanical exfoliation of fluorographite was the first method used for

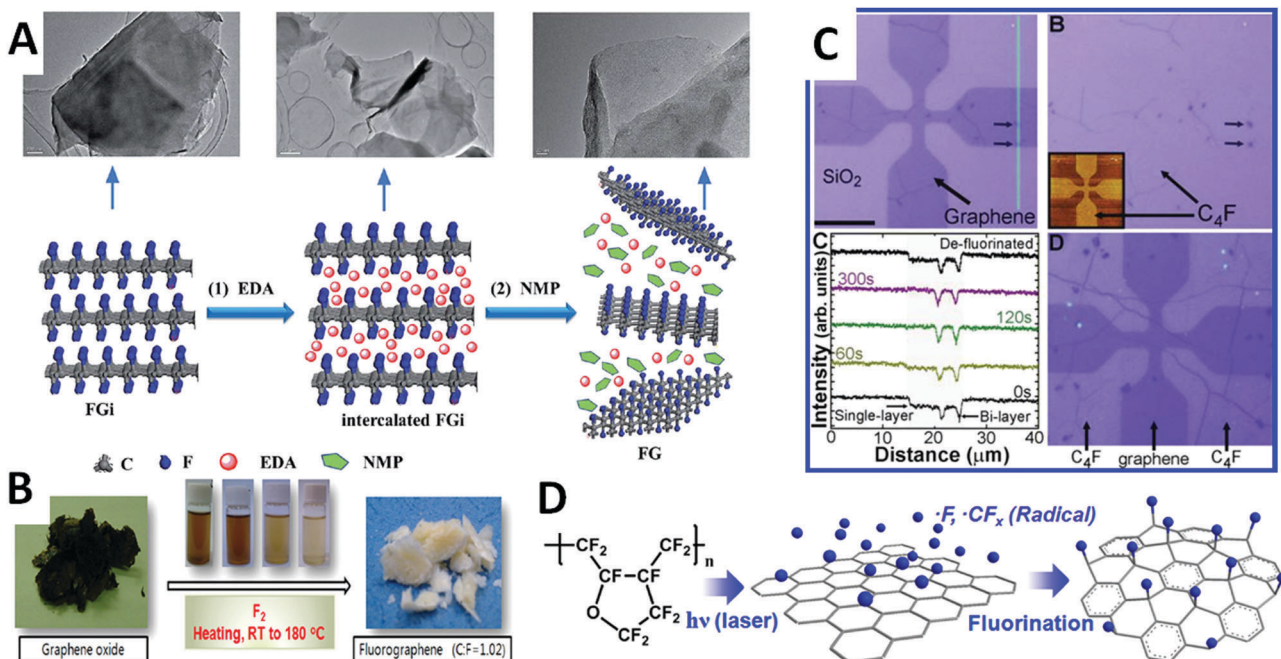


Fig. 3 (A) The preparation of fluorographene by intercalation of EDA and subsequent exfoliation by sonication at room temperature in NMP. Reproduced from ref. 73 with permission from Royal Society of Chemistry, copyright 2014. (B) Direct high temperature treatment of graphene oxide with fluorine produce high degree fluorinated graphene. Reproduced from ref. 59 with permission from American Chemical Society, copyright 2013; (C) spatially resolved fluorination of CVD growth graphene with XeF<sub>2</sub> and corresponding AFM height profiles. Reproduced from ref. 28 with permission from American Chemical Society, copyright 2010; (D) thermal decomposition of fluoropolymer producing fluorine radicals was reported as an effective method for spatially resolved fluorination of CVD growth graphene. Reproduced from ref. 72 with permission from Royal Society of Chemistry, copyright 2014.



fluorographene synthesis.<sup>30</sup> The presence of fluorine atoms covalently bonded to the graphene skeleton increase interlayer distance and the van der Waals forces holding the individual layers become even weaker in comparison with graphite. This implies that the mechanical exfoliation of fluorographite should be less energy consuming in comparison with graphene synthesis. Other procedures that allow for synthesizing bulk quantities also exist. The most useful one is shear force milling. The yield of that procedure can be further increased by the optimization of the liquid phase composition and the use of surfactants. Since first reported in 2011 by Zbořil *et al.*, several other procedures for mechanical exfoliations have been reported. All of these procedures are based on mechanical exfoliations dealing with different solvents such as sulfolane,<sup>30</sup> *N*-methyl-2-pyrrolidone,<sup>50</sup> chloroform,<sup>52</sup> isopropanol,<sup>53</sup> acetonitrile,<sup>54</sup> and various ionic liquids.<sup>50,55</sup> Mechanical exfoliation is also attributed to the intercalation of solvents used for exfoliation. Ionic liquids like 1-butyl-3-methylimidazolium bromide and *N*-methyl-2-pyrrolidone were reported as highly effective for these purposes.<sup>50,55</sup> The yield of exfoliation can be further improved by increasing temperature, typically in the range of 50–100 °C. Surfactants such as hexadecyl-trimethyl-ammonium bromide and dopamine were also used for intercalation-based exfoliation.<sup>52</sup> Methods based on the oxidation of fluorographite that led to partially fluorinated hydrophilic graphene oxide were recently reported.<sup>56,57</sup>

The chemical synthesis procedures are typically based on the reaction of graphene or its derivatives with various fluorination reagents. Fluorination was reported for bulk graphene prepared by “top-down” procedures as well as for CVD graphene. Many methods were reported for the fluorination of bulk graphene. However, only a few of them led to fully fluorinated graphene with stoichiometric composition  $C_1F_1$ .<sup>47</sup> It should also be mentioned that perfluorinated graphene can have a composition exceeding  $C_1F_1$ . This is due to the presence of  $CF_2$  and  $CF_3$  groups on the graphene edges and defect sites.<sup>58</sup> The higher concentration of such parts in combination with the small size of the graphene sheets leads to a higher excess of fluorine over stoichiometry. In order to achieve such a degree of fluorination, extremely reactive fluorination reagents must be used.<sup>58,59</sup> Fluorination of graphene oxide leads to a significantly lower F/C ratio since not only a new C–F bond must be formed, but also any remaining C–O bonds must be eliminated.<sup>60</sup> The fluorination degree (F/C ratio) was below 0.2. The resulting partially fluorinated graphene oxide remained hydrophilic after such treatment. The most typically used fluorination reagent is elemental fluorine (Fig. 3B). However, other compounds that can form elemental fluorine during reduction can be also used. The most typical example is  $XeF_2$ , which decomposes into inert xenon and fluorine molecules at elevated temperatures.<sup>27,28,42</sup> Compared to elemental fluorine, its handling is significantly less complicated. On the other hand, its high price limits its range of application, especially for bulk scale synthesis of fluorographene.<sup>27,39,42</sup> The use of  $XeF_2$  was reported for CVD-grown graphene as well as for graphene powders and assembled membranes (Fig. 3C). In the case of CVD-grown graphene, single- or both-side fluorination is obtained depending on the

graphene substrate. Since metallic substrates are typically not etched, only single-side fluorination is observed in such cases.<sup>28</sup> On the other hand, the use of a  $SiO_2/Si$  substrate can lead to both-side fluorination since  $SiO_2$  can also be etched and the other side of the graphene sheet is exposed for the reaction. Beside these two main reagents, other highly reactive compounds such as fluorine interhalogen compounds can also be used.  $ClF_3$  is an even more powerful fluorination reagent in comparison with elemental fluorine. However, its use is complicated due to its extreme reactivity and high toxicity. On the other hand, several of more mild fluorination reagents are known. The most broadly available is hydrogen fluoride and its solution in water, hydrofluoric acid. The use of hydrogen fluoride for the partial fluorination of graphene was reported by several groups.<sup>143,144</sup> Several effective fluorination reagents such as bis(2-methoxyethyl)aminosulfur trifluoride, (diethylamino)-difluorosulfonium tetrafluorido borate, and (dimethylamino)-sulfur trifluoride (DAST) are known from organic chemistry. These compounds usually need some functionalities to be present on the graphene skeleton. Therefore, graphene oxide seems to be the ideal starting material for the synthesis of partially fluorinated graphene and graphene oxide. However, these compounds are often used for the introduction of C–F bonds in organic chemistry. Their use for the formation of C–F bonds on graphene was not investigated in detail. As of now, only several works have dealt with these novel fluorination reagents like DAST.<sup>61</sup> The main advantage of these reactions is the controlled substitution of functional groups by fluorine on the graphene skeleton since only some of the functionalities can be substituted. Many other methods were reported for the general synthesis of partially fluorinated graphene and its derivatives. A typical one is the exfoliation of graphene oxide in fluorine precursors such as HF,  $SF_6$ ,  $SF_4$ , or  $MoF_6$ . Its activation can be performed through a high-temperature reaction or ion formation by plasma.<sup>145</sup> Since high temperature is applied, only a limited amount of oxygen functionalities can be found on such materials and also the concentration of fluorine is limited to several tenths of atomic percent. Use of HF under various conditions was also reported for fluorination. Aqueous solutions are typically used since handling of anhydrous hydrogen fluoride is extremely complicated and also dangerous. Fluorination of graphene oxide under hydrothermal conditions was reported with a relatively high yield of fluorination.<sup>62</sup> Also, photochemical activation of the reaction with HF was reported.<sup>63</sup> An F/C ratio of 0.39 for graphene oxide fluorinated with anhydrous  $BF_3$  etherate complex was recently reported. Also, electrochemical methods of fluorination were reported. Since this technology is well known for the synthesis of fluorinated hydrocarbons in organic chemistry, its application on graphite led to graphene with an F/C ratio of about 0.1.<sup>64</sup>

Less reactive compounds were also used for the fluorination of CVD-grown graphene. However, plasma formation is necessary to form reactive fluorine radicals and ions that can react with a graphene surface. Compared to bulk graphene, typically only up to 50% of theoretical fluorine content is obtained since the other side of the graphene sheet is attached to the substrate.



For the fluorination of CVD-grown graphene, RF plasma with gaseous reagents forming fluorine radicals like  $\text{SF}_6$  or  $\text{CF}_4$  is typically used.<sup>43,65–70</sup> More exotic methods such as an electron beam induced decomposition of  $\text{XeF}_2$  using 30 keV  $\text{Ga}^+$  ions in dual beam microscope.<sup>71</sup> The use of more reactive reagents is limited since the substrate used for graphene transfer may be significantly damaged. The gases like  $\text{CF}_4$  and  $\text{SF}_6$  are highly used in the semiconductor industry for RIE applications and the etching procedures can be relatively simply transferred for CVD-grown graphene functionalization. Site-controlled fluorination of planar graphene structures can be performed by the use of lithographic masks. Plasma-based technologies were recently used for the synthesis of fluorinated reduced graphene oxide.<sup>66,70</sup> An elegant method for the synthesis of fluorographene structures on CVD-grown graphene layers was recently published.<sup>72</sup> This method uses *in situ* local generation of a fluorine radical from localized thermal decomposition of CYTOP (a fluoropolymer that can be applied to graphene by spin coating). The method is based on local laser irradiation in which locally thermally decomposed fluorine radicals can form highly spatially resolved fluorinated graphene (Fig. 3D).<sup>72</sup> This method presents a broad application potential of fluorinated graphene in microelectronic devices since it is scalable and relatively user friendly for device fabrication even on a large scale.

Compared to graphene, its derivatives exhibit significantly higher reactivity. This opens up a new field of applications for fluorographene or graphane for the synthesis of graphene derivatives, which could not be successfully prepared directly from graphene or graphene oxide. Methods for the chemical removal of fluorine atoms from fluorographene structures were discussed in previous paragraphs. Fluorographene can also be used as a starting material for further graphene derivatization. Substitution of fluorine atoms in fluorographene by hydroxyls was recently reported as an effective method of graphene derivative synthesis.<sup>51</sup> Papers dealing with Grignard reagents were recently reported. These reactive compounds can be used for the effective introduction of aliphatic and aromatic hydrocarbon chains.<sup>74,75</sup> The introduction of an SH group on a fluorographene skeleton by substitution reaction was also reported.<sup>76</sup> Interestingly, these substitution reactions were also reported for fluorinated CVD-grown graphene. A reaction with ethylenediamine led to the introduction of an alkylamino group on a graphene surface.<sup>77</sup> Similarly, a reaction with bases led to the introduction of hydroxyl groups.<sup>78</sup> Otyepka performed theoretical calculations showing that the substitution most likely proceeded by the  $\text{S}_{\text{N}}1$  mechanism.<sup>74</sup> Substitution of fluorine indeed leads to incorporation of other groups, such as carboxyl or cyano (Fig. 4).

Reports on other graphene halogen derivatives have been significantly less frequent; only several exist to date. The main reason originates from the lower stability of the halogen derivatives with increasing halogen atom radii and decreasing electronegativity. Chlorographene was studied theoretically by several groups (Fig. 2A).<sup>31,79</sup> The synthesis of chlorinated graphene was reported by several groups. However, the chlorine concentration exceeded 10 at% in only a few cases. The thermal exfoliation of graphene oxide in a chlorine atmosphere results

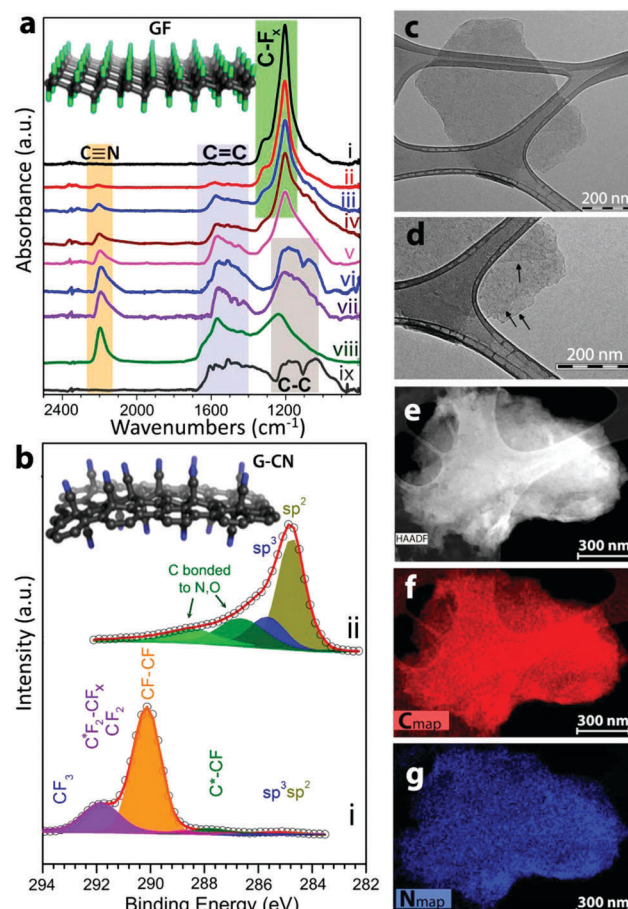


Fig. 4 Fluorographene is an excellent precursor for further functionalization, here shown as precursor for introduction of cyano groups with characterization of the resulting material. Reproduced from ref. 98 with permission from American Chemical Society, copyright 2017.

in only relatively low concentrations of chlorine, reaching about 2 at%.<sup>44</sup> Surprisingly, the use of more mild conditions and reduced temperature gives a higher degree of graphene chlorination. The synthesis procedures are typically based on radical reaction processes using elemental chlorine or its solution in inert solvents such as halogenated hydrocarbons (e.g.,  $\text{CHCl}_3$  and  $\text{CCl}_4$ ).<sup>80</sup> UV radiation for radical reactions typically originate from a mercury or xenon lamp.<sup>80,81</sup> The chlorination of graphene oxide flakes on a  $\text{SiO}_2/\text{Si}$  support using a  $\text{Cl}_2/\text{N}_2$  mixture under Xe lamp irradiation results in a chlorine concentration reaching 8 at%. Rao reported effective chlorination using liquid chlorine under UV irradiation reaching 56 wt% of Cl.<sup>46</sup> Other methods such as MW, RF, or ECR plasma treatment were also reported and were successfully employed for CVD-grown graphene.<sup>82,83</sup> The high-temperature exfoliation of graphene oxide in a chlorine atmosphere led to the formation of covalent C-Cl bonds.<sup>44</sup> However, the amount of introduced chlorine is, especially at high temperatures, relatively low due to the low stability of the C-Cl bond at high temperatures.<sup>80</sup> Friedel-Craft reactions were also used for chlorination. The chlorination of graphene edges by chlorine with  $\text{AlCl}_3$  and  $\text{ICl}$  catalysis in inert solvents was reported.<sup>84</sup> Reagents known from organic chemistry such as



thionyl chloride and sulfonyl chloride or phosphorus chlorides can also be used for selective chlorination. Use of these reagents is typically limited on modifications of more reactive graphene oxide, where chlorine derivatives of oxygen functionalities such as carboxyl chlorides can be formed. These types of reactions are of high importance for the controlled modification of graphene and its derivatives due to the formation of highly reactive acid derivatives. Highly reactive functionalities such as chlorides of carboxylic acid are then used for further chemical modifications including esterifications and many others.

The other halogengraphenes, bromographene and iodographene, usually have even lower concentrations of halogens. The interaction of graphene with bromine and formation of the C–Br bond was investigated theoretically by several authors.<sup>85–87</sup> The typical synthesis is based on the reaction of graphene oxide with elemental halogens or halogen hydrides such as hydrobromic and hydroiodic acid. High temperatures or synthesis under hydrothermal conditions are often necessary for such synthesis. The concentration of these halogens are typically lower than 10 at%. Hydrobromic acid and especially hydroiodic acid are well known for their reduction capabilities. These compounds were reported by several authors as effective reagents for the reduction of graphene oxide in bulk form as well as in the form of thin foils.<sup>88,89</sup> Compared to chloro- and fluorographene, these graphene derivatives exhibit excellent electrical conductivity.<sup>90</sup> Due to the large diameter of bromine and iodine, the electrons are delocalized and can be injected into the graphene skeleton.<sup>91</sup> Hydrobromic acid or bromine under elevated pressure and temperature or UV irradiation is typically used for the synthesis of bromographene.<sup>91,92</sup> High-temperature exfoliation of graphite oxide in a bromine atmosphere was also reported for the bromination of graphene.<sup>44</sup> Plasma processes were also effectively used for the bromination of graphene.<sup>93</sup> Effective surface bromination by plasma processes was reported for HOPG.<sup>94</sup> Bromination as well as other halogenation procedures were investigated on epitaxially grown graphene on a SiC substrate. Functionalized graphene was further used for derivatization using Grignard reagents.<sup>95</sup> Iodination of graphene has been reported in only a few papers and the yields of such reactions have been very low. Potassium iodide was reported as an effective reagent for the defluorination of fluorographene. A high-temperature/high-pressure reaction of HI and iodine with graphene oxide was reported for the iodination of graphene.<sup>96</sup> Since hydroiodic acid is an extremely efficient reducing reagent, its reaction with graphene usually leads to graphene reduction only.<sup>97</sup> Other methods are based on high-temperature exfoliation of graphite oxide in an iodine atmosphere.<sup>44</sup>

### 2.3. Crossovers – bi-component derivatives of graphene

As different halogens (and hydrogen) have different electronegativities, it is of interest to prepare well-defined mixed halogen–hydrogen and bi-halogen functionalized graphenes to tailor the properties of the material.<sup>99</sup> These “hybrid” or “crossover” halogen/hydrogen mixtures have the general formula  $C_1X_zY_{1-z}$  where X is hydrogen or halogen and Y is halogen. Fluorographane ( $C_1H_zF_{1-z}$ ) was prepared *via* a two-step process.<sup>100</sup>

Hydrogenated graphene was first prepared *via* the Birch reaction, then consequently fluorinated in a  $F_2$  atmosphere at different times and pressures. Different amounts of fluorine were introduced and it was found that with increased fluorine content the materials are more hydrophobic but exhibit faster heterogeneous electron transfer rates.<sup>101</sup> The introduction of Cl in fluorographene was carried out using the dichlorocarbene functionalization of fluorographene.<sup>102</sup>

## 3. Hydroxy and thiographene

While group VIIA (halogens) and hydrogen atoms are monovalent with carbon, neighboring group VIA (chalcogens) contains oxygen and sulphur, which readily create bonds with carbon but can be both monovalent and divalent. This can complicate the aim to prepare well-defined stoichiometric graphene derivatives unless the reaction pathway is chosen to lead to a simple monovalent derivative. The hydroboration of graphene oxide is one of the well-established synthetic chemistry routes that can be applied to create a monovalent hydroxy derivative of graphene (graphol).<sup>103</sup> Hydroboration is an addition reaction on a C=C bond that results in a H–C–C–BH<sub>2</sub> moiety. The –BH<sub>2</sub> moiety can be subsequently converted to –OH if –BH<sub>2</sub> reacts with H<sub>2</sub>O<sub>2</sub> (or to a –H bond if reacted with acid). In addition, all C=O bonds of graphene oxide react with borane and are converted to C–O–H, as shown in scheme in Fig. 5. The resulting materials had a stoichiometry of  $C_1O_{0.78}H_{0.75}$ . Graphene containing hydroxyls and also epoxide functionalities was also theoretically investigated in detail using DFT calculations.<sup>104–106</sup> Mechanochemical methods based on high-energy ball milling of graphite in the presence of potassium hydroxide were also reported for the introduction of hydroxyl groups.<sup>107</sup>

To create thiographene, an approach using graphene oxide and well established chemistry of oxygen-containing groups was undertaken. One approach was to utilize epoxy groups of GO and expose them to a ring-opening reaction to create thiol-saturated graphene oxide. This material can be subsequently applied as a nucleophile to synthesize thioether-functionalized graphene oxide.<sup>108</sup> Another approach is to use graphene oxide to convert epoxy and hydroxy groups on the graphene oxide backbone to –SH groups. This was done by reacting GO with HBr and thiourea and subsequent NaOH hydrolysis.<sup>109</sup> It should be mentioned here that the thiolation of graphene oxide is far from 100% and the resulting material is of mixed stoichiometry. A thiographene derivative can be also prepared from a well-defined precursor–fluorographene. While fluorographene was originally considered chemically inert, it was theoretically predicted that it is reactive.<sup>74</sup> Indeed, fluorographene can be converted to thiofluorographene by reacting fluorographene with HS<sup>–</sup>. The resulting C(SH)F exhibited favorable electrochemical genosensing properties when compared to fluorographene or graphene.<sup>76</sup> It should be mentioned that lower sulphur loadings are required for the induction of  $sp^3$  ferromagnetism to graphene.<sup>110</sup> However, these methods, based on high temperature exfoliation of graphene oxide in a sulfur-containing atmosphere (e.g., H<sub>2</sub>S),



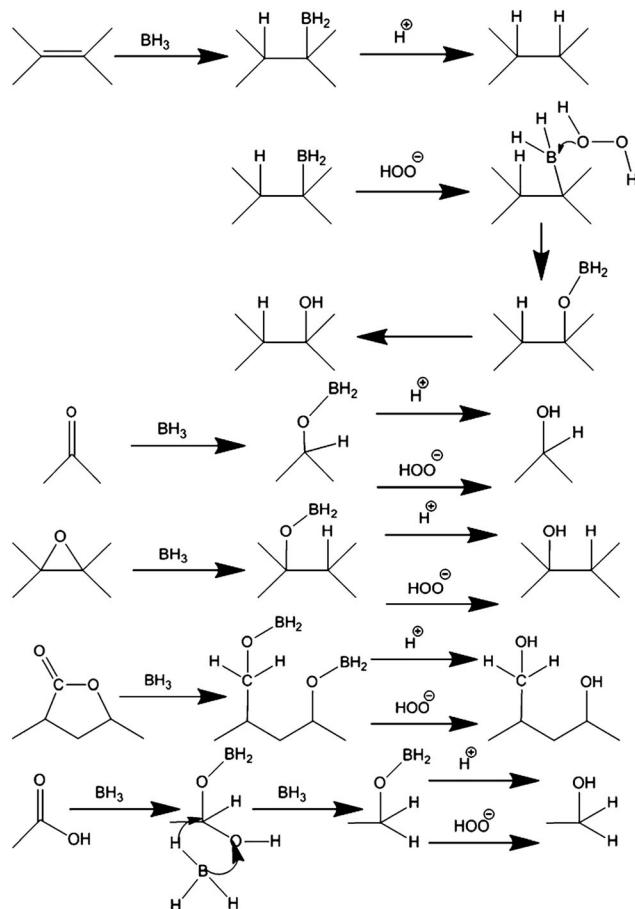


Fig. 5 Graphol. Hydroxylation of graphene oxide, if done via well-defined chemistry, can lead to hydroxylated graphene. Reproduced from ref. 103 with permission from Wiley-VCH, copyright 2015.

led to the introduction of sulfur atoms, which dominantly substituted carbon atoms on the graphene lattice and were typically not present as a thiol group. The reason for this is the high temperature employed during the synthesis.

#### 4. Carbon group-derivatized graphene (carboxy graphene)

The presence of carboxylic acid on the graphene skeleton is of pivotal importance for several applications. Hydrophilic functional groups such as carboxylic acids significantly improve the dispersibility of graphene in an aqueous environment and improve the stability of such colloidal solutions. Its presence on the graphene edges improves the mechanical properties of the graphene membrane and can be used for controlling its separation and transport properties. Carboxylic acid functionalities also strongly influence the electronic structure of graphene due to the presence of two oxygen atoms with high electronegativity. Several routes were reported for introducing carboxylic acid to the graphene. The presence of carboxylic acid also improves sorption capacity and is of high importance for environmental remediation applications.<sup>111,112</sup> The theoretical aspects of the

incorporation of  $-\text{COOH}$  group on graphene were investigated by several authors. DFT calculations show a significant impact of functionalization on morphology as well as on band-gap structure.<sup>113,114</sup> Carboxylic acid functionalities are also a suitable starting point for further graphene derivatization. Its reactivity towards amine and other groups can be used for the synthesis of more complex structures or the improvement of the mechanical properties of graphene-based composite materials. These methods are typically based on two approaches: removal of other oxygen functionalities from graphene oxide or introduction of carboxylic acid to graphene. Methods based on multiple oxidation of graphene oxide, which led to the oxidative removal of other oxygen functionalities and dominant formation of COOH groups, were recently reported.<sup>115,116</sup> On the other hand, because of the relatively high redox potential of carboxylic acid, various reducing agents can be used.<sup>117,118</sup> For example, sodium borohydride or sodium cyanoborohydride as well as several other mild reducing reagents do not reduce carboxylic acid.<sup>146</sup> This approach at reduction leaves oxygen functionalities intact. These functionalities such as hydroxyls are present in the starting material and are formed by the reduction of other oxygen functionalities. The most suitable methods, where the properties of graphene are not influenced by other functionalities, should be based on direct introduction of carboxylic acid functionalities on the graphene skeleton. The methods for direct introduction of carboxylic acid to the graphene skeleton have not been so broadly investigated, since more complicated chemical modifications have to be utilized. Carboxylic acids are typically present on the edges and defect sites of graphene, since these carbon atoms are significantly more reactive. Beside the classical chemical modifications, more exotic methods such as the mechanochemical introduction of carboxylic acid functionalities were also reported. High-energy ball milling of graphite with dry ice led to the formation of few-layered graphene with COOH functionalized edges.<sup>119</sup> A method based on Kolbe-Schmitt synthesis, which is well known in aromatic hydrocarbon chemistry, has also been reported. This method effectively introduces COOH functionalities onto the graphene surface. Otyepka was able to introduce carboxy group to fluorographene.<sup>98</sup>

#### 5. Graphene derivatives containing functional groups with nitrogen

Similarly to oxygen functionalities, nitrogen functionalities such as amino as well as azide, nitrile, and isonitrile functionalities were reported for the functionalization of graphene. Nitrogen-doped graphene was reported by several authors as a prospective catalyst for various electrochemical reactions like oxygen reduction and hydrogen evolution. However, the role of nitrogen is still not well understood and nitrogen is often present in various forms including amine as well as pyridinic and graphitic nitrogen. Other important applications are based on the reactivity of nitrogen functionalities. The azide group can be used for “click chemistry” reactions proceeding under mild conditions. Amide and nitrile functionalities can be used to increase graphene reactivity, e.g., covalent bonding of



biomolecules for sensing applications or macromolecules for composite applications.<sup>120,121</sup> These types of materials are typically obtained by heating graphene oxide or graphene at high temperature with various nitrogen precursors such as ammonia and alkylamines. In general, it is efficient to use nucleophilic substitution reactions using graphene oxide and other graphene derivatives such as fluorographene, which have significantly higher reactivity in comparison with unsubstituted graphene.<sup>122</sup> However, substitution is often accompanied with elimination.<sup>123</sup> This effect can significantly reduce the yield of the reaction or, in extreme cases, result in reduced graphene. In order to obtain material with well-defined nitrogen functionalities, low temperatures up to the solvent boiling point or synthesis under solvothermal conditions should be used. At higher temperatures (typically used for the exfoliation of graphene oxide), several different nitrogen functionalities including in-plane functionalization (e.g., pyridinic, pyrrolic, and graphitic nitrogen) are usually introduced and therefore resulting materials are poorly defined and the composition is far from stoichiometric. Classical amination, the Bucherer reaction, was reported for graphene oxide.<sup>124,125</sup> Beside the classical nucleophilic substitution reactions, other methods such as introduction of nitrile groups *via* the cycloaddition reaction with tetracyanoethylene oxide were also reported.<sup>126</sup> The functionalization of graphene oxide with isocyanate was used for the stabilization of graphene oxide in polar aprotic solvents.<sup>127</sup> Azide functional graphene sheets were used for the synthesis of nanocomposites.<sup>128</sup> However, beside the direct substitution of a graphene surface with azide functionalities, “bridge” atoms are often used and these reactive functionalities are introduced onto the graphene surface by reaction with suitable diazonium compounds by a radical reaction mechanism. Further reactions by “click” chemistry methods are not sterically hindered for further covalent attachments of large molecules.<sup>129</sup> Progress towards cyanographene was made by substitution fluorine in fluorographene (Fig. 4).<sup>98</sup> It appears that such substitutional reaction is so far the best route for well-defined nitrogen derivatized graphenes.

Graphene derivatives substituted with various nitrogen functionalities such as amines, nitriles, and azides offer a great application potential covers not only catalysis and sensing applications. Their reactivity can also be used for covalent attachments of various organic molecules for further control of graphene properties and for use as a platform for biosensing, biocatalysis, and many other applications.

## 6. Emerging applications

While there has been significant research in methodology of preparation of these graphene analogues, the applications are relatively scarce. We list here a few examples: it has been shown that introduction of hydrogen, fluoro, thio or carboxy groups can introduce ferromagnetism to the graphene sheets.<sup>11,20,110,114</sup> Hydroxyfluorographene was found to act as a room temperature ferromagnetic material.<sup>78</sup> The hydrogenated and fluorinated graphenes show faster heterogeneous electron transfer than pristine graphene, which is beneficial for electrochemical

sensing and biosensing using these materials.<sup>130,131</sup> N-Doped fluorographene was shown to act as platform for catalytic metal nanoparticles with enhanced oxygen reduction performance.<sup>132</sup> Thiofluorographene acts as selective platform for DNA detection *via* non-covalent bonding. Carboxylated graphene was covalently functionalized with single stranded DNA (ssDNA) which leads to sensitive target DNA detection.<sup>133</sup> Fluorographane was shown to have highly hydrophobic properties.<sup>134</sup> Fluorographene found its way to field effect transistors.<sup>135</sup> These are few examples of applications. There is huge potential of employing of these materials in wide variety of devices and systems.

## 7. Conclusion

Additive stoichiometric derivatives of graphene show great promise for materials science as they are supposed to be well-defined construction blocks of future devices with tailored properties. However, so far, fully  $C_1X_1$  derivatives of graphene are based on heteroatoms of the smallest size, such as hydrogen (graphane), fluorographene, and their mixed product, fluorographane. These materials exhibit interesting properties, from fluorescence to ferromagnetism. These materials serve a great precursors for further functionalization. Other prepared derivatives, such as hydroxygraphane (graphol) show a  $C_1(OH)_{0.75}$  summary formula. Similarly, thiographene has not yet been prepared in a fully saturated form  $C_1(SH)_1$ ; carboxy and cyano derivatives also do not show full coverage of graphene sheet. A question remains as to whether fully saturated graphenes are unstable, sterically prohibited, or we simply do not yet have the right synthetic approach. There are exciting possibilities in investigating these questions – from empirical as well as from theoretical points of view. Various functional groups offer different possibilities for their chemistry. Halogen groups, mainly fluorine, can be easily used as precursor for further derivatization of graphene sheets with other groups or with organic molecule handles. Cyanographene shows great potential for creation of well-defined nitro-derivatives using well-established organic chemistry procedures. Carboxy graphene allows further functionalization *via* established chemistry, *i.e.* to attach *i.e.* single stranded DNA. There is immense potential of utilization of synthetic chemistry potential to transform these well defined analogues of graphene for required applications.

## Acknowledgements

M. P. thanks to Tier 1 (1/13) for funding. Z. S. was supported by Czech Science Foundation (GACR No. 15-09001S and 16-05167S). This work was created with the financial support of the Neuron Foundation for science support.

## References

- 1 E. Fitzer, K.-H. Kochling, H. Boehm and H. Marsh, *Pure Appl. Chem.*, 1995, **67**, 473–506.
- 2 A. H. Khan, S. Ghosh, B. Pradhan, A. Dalui, L. K. Shrestha, S. Acharya and K. Ariga, *Bull. Chem. Soc. Jpn.*, 2017, **90**, 627.



3 (a) I. Shintaro, *Bull. Chem. Soc. Jpn.*, 2015, **88**, 1619–1628; (b) L. Wang and M. Pumera, *Appl. Mater. Today*, 2016, **5**, 134.

4 V. Georgakilas, J. N. Tiwari, K. C. Kemp, J. A. Perman, A. B. Bourlinos, K. S. Kim and R. Zboril, *Chem. Rev.*, 2016, **116**, 5464–5519.

5 (a) D. Higgins, P. Zamani, A. Yu and Z. Chen, *Energy Environ. Sci.*, 2016, **9**, 357–390; (b) S. Ken and A. Markus, *Bull. Chem. Soc. Jpn.*, 2015, **88**, 386–398.

6 R. K. Joshi, S. Alwarappan, M. Yoshimura, V. Sahajwalla and Y. Nishina, *Appl. Mater. Today*, 2015, **1**, 1.

7 J. O. Sofo, A. S. Chaudhari and G. D. Barber, *Phys. Rev. B: Condens. Matter Mater. Phys.*, 2007, **75**, 153401.

8 M. Pumera and C. H. A. Wong, *Chem. Soc. Rev.*, 2013, **42**, 5987–5995.

9 M. Pumera, *Chem. Soc. Rev.*, 2010, **39**, 4146–4157.

10 H. Da, Y. P. Feng and G. Liang, *J. Phys. Chem. C*, 2011, **115**, 22701–22706.

11 A. Y. S. Eng, H. L. Poh, F. Šaněk, M. Maryško, S. Matějková, Z. Sofer and M. Pumera, *ACS Nano*, 2013, **7**, 5930–5939.

12 D. Smith, R. T. Howie, I. F. Crowe, C. L. Simionescu, C. Muryn, V. Vishnyakov, K. S. Novoselov, Y.-J. Kim, M. P. Halsall, E. Gregoryanz and J. E. Proctor, *ACS Nano*, 2015, **9**, 8279–8283.

13 K. Drogowska, P. Kovaříček and M. Kalbáč, *Chem. – Eur. J.*, 2017, **23**, 4073–4078.

14 Z. Sofer, O. Jankovsky, A. Libanska, P. Simek, M. Novacek, D. Sedmidubsky, A. Mackova, R. Miksova and M. Pumera, *Nanoscale*, 2015, **7**, 10535–10543.

15 O. Jankovský, P. Šimek, J. Luxa, D. Sedmidubský, I. Tomandl, A. Macková, R. Mikšová, P. Malinský, M. Pumera and Z. Sofer, *ChemPlusChem*, 2015, **80**, 1399–1407.

16 K. S. Subrahmanyam, P. Kumar, U. Maitra, A. Govindaraj, K. P. S. S. Hembram, U. V. Waghmare and C. N. R. Rao, *Proc. Natl. Acad. Sci. U. S. A.*, 2011, **108**, 2674–2677.

17 R. A. Schäfer, J. M. Englert, P. Wehrfritz, W. Bauer, F. Hauke, T. Seyller and A. Hirsch, *Angew. Chem., Int. Ed.*, 2013, **52**, 754–757.

18 D. Bousa, J. Luxa, D. Sedmidubsky, S. Huber, O. Jankovsky, M. Pumera and Z. Sofer, *RSC Adv.*, 2016, **6**, 6475–6485.

19 L. Wang, Z. Sofer, D. Bouša, D. Sedmidubský, Š. Huber, S. Matějková, A. Michalcová and M. Pumera, *Angew. Chem.*, 2016, **128**, 14171–14175.

20 A. Y. S. Eng, Z. Sofer, Š. Huber, D. Bouša, M. Maryško and M. Pumera, *Chem. – Eur. J.*, 2015, **21**, 16828–16838.

21 X. Zhang, Y. Huang, S. Chen, N. Y. Kim, W. Kim, D. Schilter, M. Biswal, B. Li, Z. Lee, S. Ryu, C. W. Bielawski, W. S. Bacsá and R. S. Ruoff, *J. Am. Chem. Soc.*, 2016, **138**, 14980–14986.

22 C. K. Chua, Z. Sofer and M. Pumera, *Angew. Chem.*, 2016, **128**, 10909–10912.

23 A. Y. S. Eng, Z. Sofer, D. Bouša, D. Sedmidubský, Š. Huber and M. Pumera, *Adv. Funct. Mater.*, 2017, 1605797.

24 R. A. Schäfer, D. Dasler, U. Mundloch, F. Hauke and A. Hirsch, *J. Am. Chem. Soc.*, 2016, **138**, 1647–1652.

25 J. Zhou, Q. Wang, Q. Sun, X. S. Chen, Y. Kawazoe and P. Jena, *Nano Lett.*, 2009, **9**, 3867–3870.

26 S. M. Tan, Z. Sofer and M. Pumera, *Electroanalysis*, 2013, **25**, 703–705.

27 R. R. Nair, W. Ren, R. Jalil, I. Riaz, V. G. Kravets, L. Britnell, P. Blake, F. Schedin, A. S. Mayorov, S. Yuan, M. I. Katsnelson, H.-M. Cheng, W. Strupinski, L. G. Bulusheva, A. V. Okotrub, I. V. Grigorieva, A. N. Grigorenko, K. S. Novoselov and A. K. Geim, *Small*, 2010, **6**, 2877–2884.

28 J. T. Robinson, J. S. Burgess, C. E. Junkermeier, S. C. Badescu, T. L. Reinecke, F. K. Perkins, M. K. Zalalutdinov, J. W. Baldwin, J. C. Culbertson, P. E. Sheehan and E. S. Snow, *Nano Lett.*, 2010, **10**, 3001–3005.

29 D. K. Samarakoon, Z. Chen, C. Nicolas and X.-Q. Wang, *Small*, 2011, **7**, 965–969.

30 R. Zbořil, F. Karlický, A. B. Bourlinos, T. A. Steriotis, A. K. Stubos, V. Georgakilas, K. Šafářová, D. Jančík, C. Trapalis and M. Otyepka, *Small*, 2010, **6**, 2885–2891.

31 M. Yang, L. Zhou, J. Wang, Z. Liu and Z. Liu, *J. Phys. Chem. C*, 2012, **116**, 844–850.

32 J. Zheng, H.-T. Liu, B. Wu, C.-A. Di, Y.-L. Guo, T. Wu, G. Yu, Y.-Q. Liu and D.-B. Zhu, *Sci. Rep.*, 2012, **2**, 662.

33 H. Y. Liu, Z. F. Hou, C. H. Hu, Y. Yang and Z. Z. Zhu, *J. Phys. Chem. C*, 2012, **116**, 18193–18201.

34 T. Nakajima, *J. Fluorine Chem.*, 2013, **149**, 104–111.

35 G. G. Amatucci and N. Pereira, *J. Fluorine Chem.*, 2007, **128**, 243–262.

36 R. Romero-Aburto, T. N. Narayanan, Y. Nagaoka, T. Hasumura, T. M. Mitcham, T. Fukuda, P. J. Cox, R. R. Bouchard, T. Maekawa, D. S. Kumar, S. V. Torti, S. A. Mani and P. M. Ajayan, *Adv. Mater.*, 2013, **25**, 5632–5637.

37 R. R. Nair, M. Sepioni, I. L. Tsai, O. Lehtinen, J. Keinonen, A. V. Krasheninnikov, T. Thomson, A. K. Geim and I. V. Grigorieva, *Nat. Phys.*, 2012, **8**, 199–202.

38 Y. H. Hu, *Small*, 2014, **10**, 1451–1452.

39 Y. Zheng, X. Wan, N. Tang, Q. Feng, F. Liu and Y. Du, *Carbon*, 2015, **89**, 300–307.

40 X. Chia, A. Ambrosi, M. Otyepka, R. Zbořil and M. Pumera, *Chem. – Eur. J.*, 2014, **20**, 6665–6671.

41 F. Karlický and M. Otyepka, *J. Chem. Theory Comput.*, 2013, **9**, 4155–4164.

42 K.-J. Jeon, Z. Lee, E. Pollak, L. Moreschini, A. Bostwick, C.-M. Park, R. Mendelsberg, V. Radmilovic, R. Kostecki, T. J. Richardson and E. Rotenberg, *ACS Nano*, 2011, **5**, 1042–1046.

43 B. Wang, J. Wang and J. Zhu, *ACS Nano*, 2014, **8**, 1862–1870.

44 H. L. Poh, P. Šimek, Z. Sofer and M. Pumera, *Chem. – Eur. J.*, 2013, **19**, 2655–2662.

45 Z. Yao, H. Nie, Z. Yang, X. Zhou, Z. Liu and S. Huang, *Chem. Commun.*, 2012, **48**, 1027–1029.

46 K. Gopalakrishnan, K. S. Subrahmanyam, P. Kumar, A. Govindaraj and C. N. R. Rao, *RSC Adv.*, 2012, **2**, 1605–1608.

47 S. H. Cheng, K. Zou, F. Okino, H. R. Gutierrez, A. Gupta, N. Shen, P. C. Eklund, J. O. Sofo and J. Zhu, *Phys. Rev. B: Condens. Matter Mater. Phys.*, 2010, **81**, 205435.

48 O. Jankovský, V. Mazánek, K. Klímová, D. Sedmidubský, J. Kosina, M. Pumera and Z. Sofer, *Chem. – Eur. J.*, 2016, **22**, 17696–17703.



49 F. Karlický, K. Kumara Ramanatha Datta, M. Otyepka and R. Zbořil, *ACS Nano*, 2013, **7**, 6434–6464.

50 P. Gong, Z. Wang, J. Wang, H. Wang, Z. Li, Z. Fan, Y. Xu, X. Han and S. Yang, *J. Mater. Chem.*, 2012, **22**, 16950–16956.

51 P. Gong, J. Wang, W. Sun, D. Wu, Z. Wang, Z. Fan, H. Wang, X. Han and S. Yang, *Nanoscale*, 2014, **6**, 3316–3324.

52 M. Zhu, X. Xie, Y. Guo, P. Chen, X. Ou, G. Yu and M. Liu, *Phys. Chem. Chem. Phys.*, 2013, **15**, 20992–21000.

53 L. Zhan, S. Yang, Y. Wang, Y. Wang, L. Ling and X. Feng, *Adv. Mater. Interfaces*, 2014, **1**, 1300149.

54 C. Sun, Y. Feng, Y. Li, C. Qin, Q. Zhang and W. Feng, *Nanoscale*, 2014, **6**, 2634–2641.

55 H. Chang, J. Cheng, X. Liu, J. Gao, M. Li, J. Li, X. Tao, F. Ding and Z. Zheng, *Chem. – Eur. J.*, 2011, **17**, 8896–8903.

56 A. Mathkar, T. N. Narayanan, L. B. Alemany, P. Cox, P. Nguyen, G. Gao, P. Chang, R. Romero-Aburto, S. A. Mani and P. M. Ajayan, *Part. Part. Syst. Charact.*, 2013, **30**, 266–272.

57 P. Chantharasupawong, R. Philip, N. T. Narayanan, P. M. Sudeep, A. Mathkar, P. M. Ajayan and J. Thomas, *J. Phys. Chem. C*, 2012, **116**, 25955–25961.

58 V. Mazanek, O. Jankovsky, J. Luxa, D. Sedmidubsky, Z. Janousek, F. Semenza, M. Mikulics and Z. Sofer, *Nanoscale*, 2015, **7**, 13646–13655.

59 X. Wang, Y. Dai, J. Gao, J. Huang, B. Li, C. Fan, J. Yang and X. Liu, *ACS Appl. Mater. Interfaces*, 2013, **5**, 8294–8299.

60 O. Jankovsky, P. Simek, D. Sedmidubsky, S. Matejkova, Z. Janousek, F. Semenza, M. Pumera and Z. Sofer, *RSC Adv.*, 2014, **4**, 1378–1387.

61 X. Gao and X. S. Tang, *Carbon*, 2014, **76**, 133–140.

62 Z. Wang, J. Wang, Z. Li, P. Gong, X. Liu, L. Zhang, J. Ren, H. Wang and S. Yang, *Carbon*, 2012, **50**, 5403–5410.

63 P. Gong, Z. Wang, Z. Li, Y. Mi, J. Sun, L. Niu, H. Wang, J. Wang and S. Yang, *RSC Adv.*, 2013, **3**, 6327–6330.

64 M. Bruna, B. Massessi, C. Cassiago, A. Battiato, E. Vittone, G. Speranza and S. Borini, *J. Mater. Chem.*, 2011, **21**, 18730–18737.

65 M. Baraket, S. G. Walton, E. H. Lock, J. T. Robinson and F. K. Perkins, *Appl. Phys. Lett.*, 2010, **96**, 231501.

66 S. B. Bon, L. Valentini, R. Verdejo, J. L. Garcia Fierro, L. Peponi, M. A. Lopez-Manchado and J. M. Kenny, *Chem. Mater.*, 2009, **21**, 3433–3438.

67 G. Bruno, G. V. Bianco, M. M. Giangregorio, M. Losurdo and P. Capezzuto, *Phys. Chem. Chem. Phys.*, 2014, **16**, 13948–13955.

68 K.-I. Ho, J.-H. Liao, C.-H. Huang, C.-L. Hsu, W. Zhang, A.-Y. Lu, L.-J. Li, C.-S. Lai and C.-Y. Su, *Small*, 2014, **10**, 989–997.

69 S. D. Sherpa, J. Kunc, Y. Hu, G. Levitin, W. A. D. Heer, C. Berger and D. W. Hess, *Appl. Phys. Lett.*, 2014, **104**, 081607.

70 X. Yu, K. Lin, K. Qiu, H. Cai, X. Li, J. Liu, N. Pan, S. Fu, Y. Luo and X. Wang, *Carbon*, 2012, **50**, 4512–4517.

71 H. Li, L. Daukiya, S. Haldar, A. Lindblad, B. Sanyal, O. Eriksson, D. Aubel, S. Hajjar-Garreau, L. Simon and K. Leifer, *Sci. Rep.*, 2016, **6**, 19719.

72 W. H. Lee, J. W. Suk, H. Chou, J. Lee, Y. Hao, Y. Wu, R. Piner, D. Akinwande, K. S. Kim and R. S. Ruoff, *Nano Lett.*, 2012, **12**, 2374–2378.

73 K. Hou, P. Gong, J. Wang, Z. Yang, Z. Wang and S. Yang, *RSC Adv.*, 2014, **4**, 56543–56551.

74 (a) M. Dubecký, E. Otyepková, P. Lazar, F. Karlický, M. Petr, K. Čepe, P. Banáš, R. Zbořil and M. Otyepka, *J. Phys. Chem. Lett.*, 2015, **6**, 1430–1434; (b) E. Otyepková, P. Lazar, K. Čepe, O. Tomanec and M. Otyepka, *Appl. Mater. Today*, 2016, **5**, 142.

75 V. Mazánek, A. Libánská, J. Štrála, D. Bouša, D. Sedmidubský, M. Pumera, Z. Janoušek, J. Plutnar and Z. Sofer, *Chem. – Eur. J.*, 2017, **23**, 1956–1964.

76 V. Urbanová, K. Holá, A. B. Bourlinos, K. Čepe, A. Ambrosi, A. H. Loo, M. Pumera, F. Karlický, M. Otyepka and R. Zbořil, *Adv. Mater.*, 2015, **27**, 2305–2310.

77 R. Stine, J. W. Ciszek, D. E. Barlow, W.-K. Lee, J. T. Robinson and P. E. Sheehan, *Langmuir*, 2012, **28**, 7957–7961.

78 J. Tuček, K. Holá, A. B. Bourlinos, P. Błoński, A. Bakandritsos, J. Ugolotti, M. Dubecký, F. Karlický, V. Ranc, K. Čepe, M. Otyepka and R. Zbořil, *Nat. Commun.*, 2017, **8**, 14525.

79 H. Şahin and S. Ciraci, *J. Phys. Chem. C*, 2012, **116**, 24075–24083.

80 D. Bousa, J. Luxa, V. Mazanek, O. Jankovsky, D. Sedmidubsky, K. Klimova, M. Pumera and Z. Sofer, *RSC Adv.*, 2016, **6**, 66884–66892.

81 B. Li, L. Zhou, D. Wu, H. Peng, K. Yan, Y. Zhou and Z. Liu, *ACS Nano*, 2011, **5**, 5957–5961.

82 X. Zhang, A. Hsu, H. Wang, Y. Song, J. Kong, M. S. Dresselhaus and T. Palacios, *ACS Nano*, 2013, **7**, 7262–7270.

83 X. Zhang, T. Schiros, D. Nordlund, Y. C. Shin, J. Kong, M. Dresselhaus and T. Palacios, *Adv. Funct. Mater.*, 2015, **25**, 4163–4169.

84 Y.-Z. Tan, B. Yang, K. Parvez, A. Narita, S. Osella, D. Beljonne, X. Feng and K. Müllen, *Nat. Commun.*, 2013, **4**, 2646.

85 A. Yaya, C. P. Ewels, I. Suarez-Martinez, P. Wagner, S. Lefrant, A. Okotrub, L. Bulusheva and P. R. Briddon, *Phys. Rev. B: Condens. Matter Mater. Phys.*, 2011, **83**, 045411.

86 A. N. Rudenko, F. J. Keil, M. I. Katsnelson and A. I. Lichtenstein, *Phys. Rev. B: Condens. Matter Mater. Phys.*, 2010, **82**, 035427.

87 X. Fan, L. Liu, J.-L. Kuo and Z. Shen, *J. Phys. Chem. C*, 2010, **114**, 14939–14945.

88 C. K. Chua and M. Pumera, *J. Mater. Chem.*, 2012, **22**, 23227–23231.

89 S. Pei, J. Zhao, J. Du, W. Ren and H.-M. Cheng, *Carbon*, 2010, **48**, 4466–4474.

90 O. Jankovsky, P. Simek, K. Klimova, D. Sedmidubsky, S. Matejkova, M. Pumera and Z. Sofer, *Nanoscale*, 2014, **6**, 6065–6074.



91 A. E. Mansour, S. Dey, A. Amassian and M. H. Tanielian, *ACS Appl. Mater. Interfaces*, 2015, **7**, 17692–17699.

92 Y. Li, H. Chen, L. Y. Voo, J. Ji, G. Zhang, G. Zhang, F. Zhang and X. Fan, *J. Mater. Chem.*, 2012, **22**, 15021–15024.

93 J. F. Friedrich, G. Hidde, A. Lippitz and W. E. S. Unger, *Plasma Chem. Plasma Process.*, 2014, **34**, 621–645.

94 A. Lippitz, J. F. Friedrich and W. E. S. Unger, *Surf. Sci.*, 2013, **611**, L1–L7.

95 M. Z. Hossain and M. B. A. Razak, *New J. Chem.*, 2016, **40**, 1671–1678.

96 P. Simek, K. Klimova, D. Sedmidubsky, O. Jankovsky, M. Pumera and Z. Sofer, *Nanoscale*, 2015, **7**, 261–270.

97 Z. Wang, W. Wang, M. Wang, X. Meng and J. Li, *J. Mater. Sci.*, 2013, **48**, 2284–2289.

98 A. Bakandritsos, M. Pykal, P. Błoński, P. Jakubec, D. D. Chronopoulos, K. Poláková, V. Georgakilas, K. Čepé, O. Tomanec, V. Ranc, A. B. Bourlinos, R. Zbořil and M. Otyepka, *ACS Nano*, 2017, **11**, 2982–2991.

99 R. Paupitz, P. A. Autreto, S. Legoaas, S. G. Srinivasan, A. C. van Duin and D. Galvao, *Nanotechnology*, 2012, **24**, 035706.

100 Z. Sofer, P. Simek, V. Mazanek, F. Semenza, Z. Janousek and M. Pumera, *Chem. Commun.*, 2015, **51**, 5633–5636.

101 R. Gusmão, Z. Sofer, F. Šembera, Z. Janoušek and M. Pumera, *Chem. – Eur. J.*, 2015, **21**, 16474–16478.

102 P. Lazar, C. K. Chua, K. Holá, R. Zbořil, M. Otyepka and M. Pumera, *Small*, 2015, **11**, 3790–3796.

103 H. L. Poh, Z. Sofer, P. Šimek, I. Tomandl and M. Pumera, *Chem. – Eur. J.*, 2015, **21**, 8130–8136.

104 J.-A. Yan and M. Y. Chou, *Phys. Rev. B: Condens. Matter Mater. Phys.*, 2010, **82**, 125403.

105 A. Bagri, R. Grantab, N. V. Medhekar and V. B. Shenoy, *J. Phys. Chem. C*, 2010, **114**, 12053–12061.

106 N. Ghaderi and M. Peressi, *J. Phys. Chem. C*, 2010, **114**, 21625–21630.

107 L. Yan, M. Lin, C. Zeng, Z. Chen, S. Zhang, X. Zhao, A. Wu, Y. Wang, L. Dai, J. Qu, M. Guo and Y. Liu, *J. Mater. Chem.*, 2012, **22**, 8367–8371.

108 H. R. Thomas, A. J. Marsden, M. Walker, N. R. Wilson and J. P. Rourke, *Angew. Chem., Int. Ed.*, 2014, **53**, 7613–7618.

109 C. K. Chua and M. Pumera, *ACS Nano*, 2015, **9**, 4193–4199.

110 J. Tuček, P. Błoński, Z. Sofer, P. Šimek, M. Petr, M. Pumera, M. Otyepka and R. Zbořil, *Adv. Mater.*, 2016, **28**, 5045–5053.

111 S. Park, K.-S. Lee, G. Bozoklu, W. Cai, S. T. Nguyen and R. S. Ruoff, *ACS Nano*, 2008, **2**, 572–578.

112 K. Klímová, M. Pumera, J. Luxa, O. Jankovský, D. Sedmidubský, S. Matějková and Z. Sofer, *J. Phys. Chem. C*, 2016, **120**, 24203–24212.

113 N. Al-Aqtash and I. Vasiliev, *J. Phys. Chem. C*, 2009, **113**, 12970–12975.

114 A. Y. S. Eng, Z. Sofer, D. Sedmidubský and M. Pumera, *ACS Nano*, 2017, **11**, 1789–1797.

115 M. Novacek, O. Jankovsky, J. Luxa, D. Sedmidubsky, M. Pumera, V. Fila, M. Lhotka, K. Klimova, S. Matejkova and Z. Sofer, *J. Mater. Chem. A*, 2017, **5**, 2739–2748.

116 O. Jankovský, M. Nováček, J. Luxa, D. Sedmidubský, V. Fila, M. Pumera and Z. Sofer, *Chem. – Eur. J.*, 2016, **22**, 17416–17424.

117 C. Xu, R. Yuanm and X. Wang, *New Carbon Mater.*, 2014, **29**, 61–66.

118 J. Zhang, H. Yang, G. Shen, P. Cheng, J. Zhang and S. Guo, *Chem. Commun.*, 2010, **46**, 1112–1114.

119 I.-Y. Jeon, Y.-R. Shin, G.-J. Sohn, H.-J. Choi, S.-Y. Bae, J. Mahmood, S.-M. Jung, J.-M. Seo, M.-J. Kim, D. Wook Chang, L. Dai and J.-B. Baek, *Proc. Natl. Acad. Sci. U. S. A.*, 2012, **109**, 5588–5593.

120 Y. Zhan, X. Yang, H. Guo, J. Yang, F. Meng and X. Liu, *J. Mater. Chem.*, 2012, **22**, 5602–5608.

121 Y. Zhan, J. Yang, Y. Zhou, X. Yang, F. Meng and X. Liu, *Mater. Lett.*, 2012, **78**, 88–91.

122 C. Bosch-Navarro, M. Walker, N. R. Wilson and J. P. Rourke, *J. Mater. Chem. C*, 2015, **3**, 7627–7631.

123 K. E. Whitener, R. Stine, J. T. Robinson and P. E. Sheehan, *J. Phys. Chem. C*, 2015, **119**, 10507–10512.

124 A. Navaee and A. Salimi, *RSC Adv.*, 2015, **5**, 59874–59880.

125 C. K. Chua, Z. Sofer, J. Luxa and M. Pumera, *Chem. – Eur. J.*, 2015, **21**, 8090–8095.

126 X. Peng, Y. Li, G. Zhang, F. Zhang and X. Fan, *J. Nanomater.*, 2013, **2013**, 841789.

127 S. Stankovich, R. D. Piner, S. T. Nguyen and R. S. Ruoff, *Carbon*, 2006, **44**, 3342–3347.

128 N. R. Han and J. W. Cho, *Composites, Part A*, 2016, **87**, 78–85.

129 M. Castelaín, G. Martínez, P. Merino, J. Á. Martín-Gago, J. L. Segura, G. Ellis and H. J. Salavagione, *Chem. – Eur. J.*, 2012, **18**, 4965–4973.

130 H. L. Poh, Z. Sofer and M. Pumera, *Electrochim. Commun.*, 2012, **25**, 58–61.

131 V. Urbanova, F. Karlicky, A. Matej, F. Semenza, Z. Janousek, J. A. Perman, V. Ranc, K. Cepe, J. Michl, M. Otyepka and R. Zboril, *Nanoscale*, 2016, **8**, 12134–12142.

132 T. V. Vineesh, M. A. Nazrulla, S. Krishnamoorthy, T. N. Narayanan and S. Alwarappan, *Appl. Mater. Today*, 2015, **1**, 74–79.

133 A. Bonanni, C. K. Chua and M. Pumera, *Chem. – Eur. J.*, 2014, **20**, 217–222.

134 Z. Sofer, P. Simek, V. Mazanek, F. Semenza, Z. Janousek and M. Pumera, *Chem. Commun.*, 2015, **51**, 5633–5636.

135 K.-I. Ho, M. Boutchich, C.-Y. Su, R. Moreddu, E. S. R. Marianathan, L. Montes and C.-S. Lai, *Adv. Mater.*, 2015, **27**, 6519–6525.

136 T. Szabo, O. Berkesi, P. Forgo, K. Josepovits, Y. Sanakis, D. Petridis and I. Dékány, *Chem. Mater.*, 2006, **18**, 2740.

137 C. K. Chua, Z. Sofer and M. Pumera, *Chem. – Eur. J.*, 2012, **18**, 13453.

138 D. C. Elias, R. R. Nair, T. M. G. Mohiuddin, S. V. Morozov, P. Blake, M. P. Halsall, A. C. Ferrari, D. W. Boukhvalov, M. I. Katsnelson, A. K. Geim and K. S. Novoselov, *Science*, 2009, **323**, 610.



139 J. S. Burgess, B. R. Matis, J. T. Robinson, F. A. Bulat, F. K. Perkins, B. H. Houston and J. W. Baldwin, *Carbon*, 2011, **49**, 4420.

140 H. Kim, T. Balgar and E. Hasselbrink, *Chem. Phys. Lett.*, 2012, **546**, 12–17.

141 A. Y. S. Eng, Z. Sofer, P. Simek, J. Kosina and M. Pumera, *Chem. – Eur. J.*, 2013, **19**, 15583.

142 H. L. Poh, F. Šaněk, Z. Sofer and M. Pumera, *Nanoscale*, 2012, **4**, 7006.

143 N. A. Nebogatikova, I. V. Antonova, V. A. Volodin and V. Ya. Prinz, *Phys. E*, 2013, **52**, 106–111.

144 N. A. Nebogatikova, V. Antonova, V. Ya. Prinz, V. A. Volodin, D. A. Zatsepin, E. Z. Kurmaev, I. S. Zhidkov and S. O. Cholakh, *Nanotechnol. Russ.*, 2014, **9**, 51–59.

145 H. L. Poh, Z. Sofer, K. Klímová and M. Pumera, *J. Mater. Chem. C*, 2014, **2**, 5198–5204.

146 C. K. Chua and M. Pumera, *J. Mater. Chem. A*, 2013, **1**, 1892–1898.

